Complexity in the Decomposition of Formic Acid on the TiO_2(110) Surface

Michael A. Henderson[†]

Materials and Interfaces Group, Environmental Molecular Sciences Laboratory, Pacific Northwest National Laboratory,[‡] *P.O. Box 999, MS K2-12, Richland, Washington 99352*

Received: May 22, 1996; In Final Form: September 6, 1996[⊗]

The decomposition of formic acid on the TiO_2(110) surface was examined with temperature-programmed desorption (TPD), static secondary ion mass spectrometry (SSIMS), and high-resolution electron energy loss spectroscopy (HREELS). Formic acid decomposed upon adsorption on TiO_2(110) at 110 K to formate and a proton. The formate species was identified in HREELS by the symmetric O−C−O stretching mode at 1365 cm^{-1} and the C−H stretching mode at 2920 cm^{-1}. The deposited acid proton was difficult to detect in HREELS but presumably formed a hydroxyl group at a bridging two-coordinate O^{2-} site. TPD indicated that the major formic acid decomposition products were CO and H_2O, suggestive of a dehydration process. However, a dehydration mechanism is unsuitable for describing the decomposition of formic acid on TiO_2(110) because the CO and H_2O products were formed from independent sources and by independent surface processes. CO desorbed during decomposition of formate between 400 and 700 K, but the majority of the desorbing H_2O resulted from condensation of bridging hydroxyl groups below 500 K with virtually no water desorbed during formate decomposition. Condensation of bridging hydroxyl groups left a disordered surface consisting of oxygen vacancies and adsorbed formate species. The decomposition of formate was not a straightforward process. Although CO was the major formate decomposition product, formaldehyde desorbed at 548 K as the major hydrogen-containing product, with formic acid (from formate disproportionation), water, and acetylene as additional hydrogen-containing products. Carbon dioxide desorption was also detected and coincided with formaldehyde desorption. The production of formaldehyde probably involved the oxygen vacancies produced below 500 K during water desorption. TPD results from $HC^{16}O^{16}OH$ decomposition on the ^{18}O-enriched TiO_2(110) surface indicated that oxygen exchange between the surface and the formic acid adlayer resulted in significant amounts ^{18}O-containing TPD products (carbon monoxide, water, and formaldehyde). Analysis of the desorption rates for the two carbon monoxide species revealed that $C^{18}O$ production occurred with a higher activation barrier (75 kJ/mol) than did $C^{16}O$ (52 kJ/mol). SSIMS results indicated that oxygen exchange occurred between the surface and some adsorbed formate species at temperatures as low as 400 K. These findings reveal that the decomposition of formic acid on TiO_2(110) is complex and cannot adequately be described by a simple dehydration mechanism.

1. Introduction

Although formic acid is the simplest of carboxylic acids, its surface chemistry on TiO_2 single-crystal surfaces[1−7] is complex. Formic acid decomposes on TiO_2 to produce a surface formate intermediate.[8,9] Formate, in turn, decomposes to a variety of products, the dominant of which are reported to be CO, CO_2, H_2O, and H_2. Given these products, the decomposition of formic acid on TiO_2 has frequently been described in terms of dehydration (to CO and H_2O) and dehydrogenation (to CO_2 and H_2) mechanisms.[2−5,8,10,11] These descriptions adequately reflect the overall stoichiometry of formic acid decomposition and apply well mechanistically to formic acid decomposition on most metals[12] and on some oxides.[13−16] However, results from this study suggest that the dehydration and dehydrogenation descriptions are inappropriate for characterizing formic acid decomposition on TiO_2(110). Instead, formic acid decomposition involves a complex set of chemical processes that include water formation and creation of oxygen vacancies by the reaction of the acid proton with the oxide lattice, interaction of formate with the oxygen vacancies leading to a variety of minor decomposition products, including formaldehyde, and the facile exchange of lattice oxygen into formate during its decomposition. Many of these findings were also noted in a previous study of formic acid decomposition on the {110}-microfaceted surface of TiO_2(100).[6] However, understanding the chemistry of formic acid on the {110}-microfacets of that surface was somewhat complicated by the variety of surface sites present. Therefore, the chemistry of formic acid on the TiO_2(110) surface was examined in an effort to better understand carboxylic acid chemistry on TiO_2.

2. Experimental Section

The ultrahigh vacuum chamber and experimental methods used in this study are discussed in more detail elsewhere.[17] Mounting and cleaning of the TiO_2(110) crystal have also been discussed in a previous work.[18] The temperature ramp rate for all temperature-programmed desorption (TPD) and temperature-programmed static secondary ion mass spectrometry (SSIMS) experiments was 2 K/s. TPD traces were Fourier filtered, and background signals were stripped to enhance the appearance of the data. Details regarding the Fourier deconvolution of high-resolution electron energy loss spectroscopy (HREELS) data can also be found elsewhere.[18]

Formic acid was dosed on the TiO_2(110) surface through a translatable directional doser.[17] Formic acid (HCOOH, A.C.S. reagent grade, 96% purity) was obtained from Aldrich. The

[†] Telephone: (509) 375-5970. Fax: (509) 375-5965. E-mail: ma_henderson@pnl.gov.

[‡] Pacific Northwest National Laboratory is a multiprogram national laboratory operated for the U.S. Department of Energy by Battelle Memorial Institute under Contract DE-AC06-76RLO 1830.

[⊗] Abstract published in *Advance ACS Abstracts,* December 1, 1996.

S1089-5647(96)01494-0 CCC: $14.00

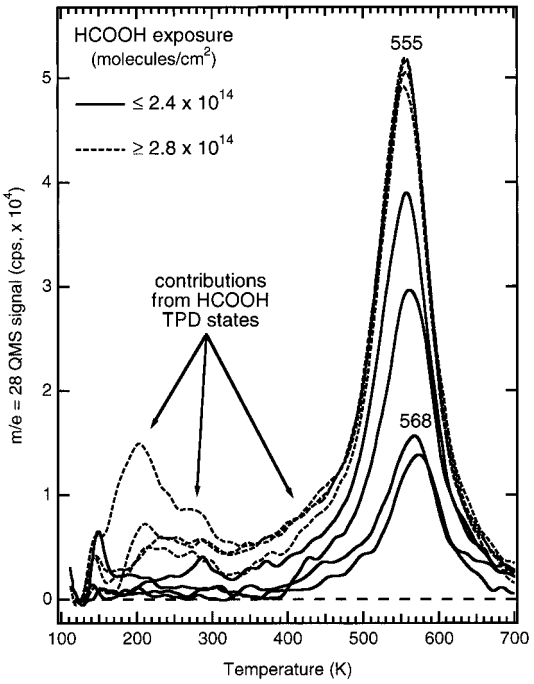

Figure 1. CO TPD from HCOOH decomposition on TiO_2(110). HCOOH exposures were 0.2, 0.5, 1.1, 2.4, 2.8, 3.2, 4.1, and 5.2 × 10^{14} molecules/cm^2.

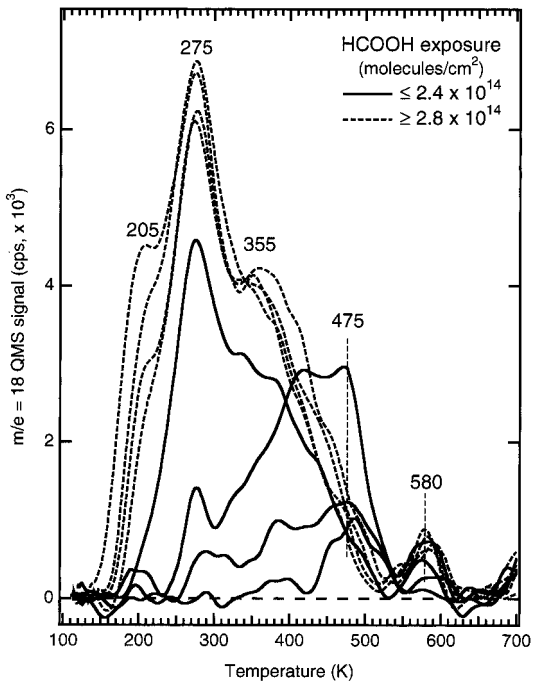

Figure 2. H_2O TPD from HCOOH decomposition on TiO_2(110). HCOOH exposures were 0.2, 0.5, 1.1, 2.4, 2.8, 3.2, 4.1, and 5.2 × 10^{14} molecules/cm^2.

major impurities, according to the supplier, were acetic acid (<0.4%) and water. Freeze−pump−thaw cycles with liquid nitrogen were performed on the formic acid before use. Additionally, the gas-handling system and doser assembly were conditioned to new exposures of formic acid at the beginning of each day.

3. Results and Discussion

3.1. TPD and HREELS Results. The thermal decomposition properties of formic acid on the TiO_2(110) surface were similar to those previously observed from the {110}-microfaceted TiO_2(100) surface.[6] The major decomposition products from both surfaces were CO and H_2O, with H_2CO, C_2H_2, and CO_2 as minor products. No H_2 was observed from either surface. Figures 1−3 show TPD results from CO, H_2O, and H_2CO desorption, respectively, as a function of HCOOH exposure. In these figures, TPD traces from HCOOH exposures greater than or equal to 2.8 × 10^{14} molecules/cm^2 are shown as dashed lines. As will be shown below, this exposure corresponds roughly to the point at which HCOOH saturates the first layer on TiO_2(110).

Figure 1 shows a series of CO TPD traces (m/e = 28) resulting from HCOOH decomposition on TiO_2(110). Desorption states in these m/e = 28 traces below 450 K resulted from quadrupole mass spectrometer (QMS) cracking of HCOOH (see below). CO, however, desorbed in a single TPD state at 555 K resulting from decomposition of the surface formate species. This CO desorption state was reaction-limited because adsorbed CO does not remain on TiO_2(110) above 150 K in ultrahigh vacuum (UHV). Although the peak temperature of this TPD state was slightly higher for low HCOOH exposures (≤0.5 × 10^{14} molecules/cm^2), the desorption process appeared to be near first order. The CO TPD peak was narrower (85 K fwhm) than that observed from the {110}-microfaceted TiO_2(100) surface (128 K fwhm) but comparable to that observed from the fully oxidized (1 × 1) TiO_2(100) surface.[6]

Figure 2 shows H_2O TPD spectra (m/e = 18) resulting from HCOOH decomposition on TiO_2(110). At low HCOOH exposures (≤0.2 × 10^{14} molecules/cm^2) the major H_2O desorption state was at 475 K. This TPD state broadened and shifted to lower temperature as the HCOOH exposure was increased. The 475 K TPD peak diminished as the HCOOH exposure was increased to 2.4 × 10^{14} molecules/cm^2, at which point most of the water desorption from HCOOH decomposition occurred below 400 K. This shift in water desorption from above 400 K to below 400 K occurred at a HCOOH exposure just prior to saturation of the monolayer (at about (2.4−2.8) × 10^{14} molecules/cm^2). In addition to the 475 K TPD state, other water TPD states were observed at about 580 K (trailing the CO TPD from formate decomposition) between 350 and 400 K and between 250 and 300 K. The 580 K state was coincident with the trace C_2H_2 product (not shown). The H_2O TPD state

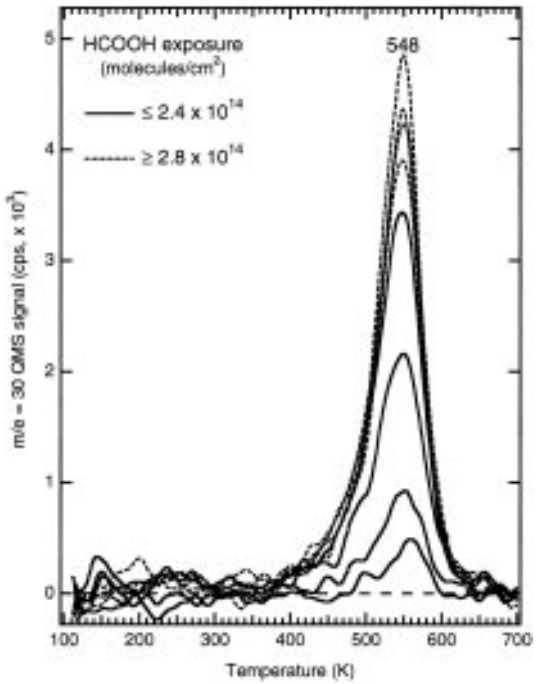

Figure 3. H_2CO TPD from HCOOH decomposition on TiO_2(110). HCOOH exposures were 0.2, 0.5, 1.1, 2.4, 2.8, 3.2, 4.1, and 5.2 × 10^{14} molecules/cm^2.

between 350 and 400 K increased in intensity and shifted slightly to lower temperature as the monolayer was saturated with HCOOH. The 250−300 K TPD state increased in intensity as a function of increasing HCOOH exposure and became resolved at 275 K. This TPD state resembled that for molecular water desorption from clean TiO_2(110).[18,19] TPD results from decomposition of $HC^{16}O^{16}OH$ on the ^{18}O-enriched TiO_2(110) surface, discussed below, show significant incorporation of ^{18}O into the water desorption product, suggesting that the lattice oxygen atoms are involved in the formation of water.

Exposures of HCOOH above 2.8×10^{14} molecules/cm^2 resulted first in the appearance of a water TPD state at about 205 K and then a TPD state at 160 K (not shown). The former state was probably due to desorption of second layer water (i.e., water hydrogen-bonded to two-coordinate O^{2-} sites[18,19]), and the latter due to water desorption from a formic acid multilayer. These two low-temperature water desorption states more than likely resulted from small amounts of water dosed with HCOOH, presumably as a result of HCOOH decomposition on the doser walls or as an impurity in the source material (see Experimental Section). Some of the H_2O TPD intensity in the 275 K TPD state probably also resulted from dosed water, as will be shown below. It is also possible that some of the water in the low-temperature TPD states resulted from a bimolecular reaction of formic acid to form formyl anhydride (reaction 1):

$$2HCOOH \rightarrow HC(=O)-O-(O=)CH + H_2O \qquad (1)$$

This reaction has been observed during formic acid adsorption on Ni(111),[20] but at present there is no direct spectroscopic evidence for it on TiO_2(110). Regardless of the source, the influence of water on HCOOH chemistry was probably negligible based on results from the coadsorption of these species on TiO_2(100).[6]

Figure 3 shows TPD spectra for formaldehyde (H_2CO) desorption from HCOOH decomposition on TiO_2(110). As was the case for the {110}-microfaceted surface of TiO_2(100), H_2CO production from HCOOH decomposition on TiO_2(110) occurred at a slightly lower peak temperature than that of the CO desorption state. In this case H_2CO desorbed at 548 K. This product, however, was not observed by Onishi and co-workers in their examination of formic acid decomposition on TiO_2(110).[4] Although an estimate of the amount of H_2CO produced was not made, the desorption signals were an order of magnitude smaller than those for CO, suggesting that H_2CO was a secondary product in the decomposition of surface formate. Based on results from Barteau and co-workers for formic acid decomposition on various surface phases of TiO_2-(001),[2,7] formaldehyde production on TiO_2(110) can be linked to the presence of either reduced Ti cation sites (e.g., Ti^{3+}) or low-coordination Ti^{4+} sites. An ideal, fully oxidized TiO_2(110) surface possesses neither of these types of sites. The inherent concentration of surface defects on the crystal used in this study was low based on previous TPD work with water.[18] Therefore, it appears that formic acid chemistry on TiO_2(110) produced the defect sites required to convert formate to formaldehyde. This effect will be discussed to a greater extent below.

A variety of molecular HCOOH desorption states were observed as a function of HCOOH exposure on TiO_2(110) (Figure 4). At very low exposures ($<0.5 \times 10^{14}$ molecules/cm^2), little or no HCOOH desorption was observed, indicating that virtually all adsorbed HCOOH molecules irreversibly decomposed upon adsorption or during TPD. A weak HCOOH desorption state was observed at about 450 K for HCOOH exposures above 0.5×10^{14} molecules/cm^2. Note that this state desorbed coincident with that of water desorption from the same HCOOH exposure (Figure 2). The 450 K state increased in intensity and shifted to lower temperature with increasing HCOOH exposures in the same manner as did the water TPD. Two new HCOOH TPD states appeared after an exposure of 2.4×10^{14} molecules/cm^2, one at higher temperature (538 K) and one at lower temperature (280 K). HREELS data (to be discussed) will show that HCOOH desorption above 250 K resulted from the recombination of surface formates with surface hydroxyl groups. Above an exposure of about 2.8×10^{14} molecules/cm^2 subsequently dosed HCOOH molecules desorbed first in a TPD state that shifted from 220 to 197 K with increasing exposure and then in a TPD state at 164 K. The latter TPD state was due to multilayer desorption.[21−23] Comparison of Figure 4 with Figure 1 supports the argument that the $m/e = 28$ features indicated in Figure 1 were due to formic acid desorption.

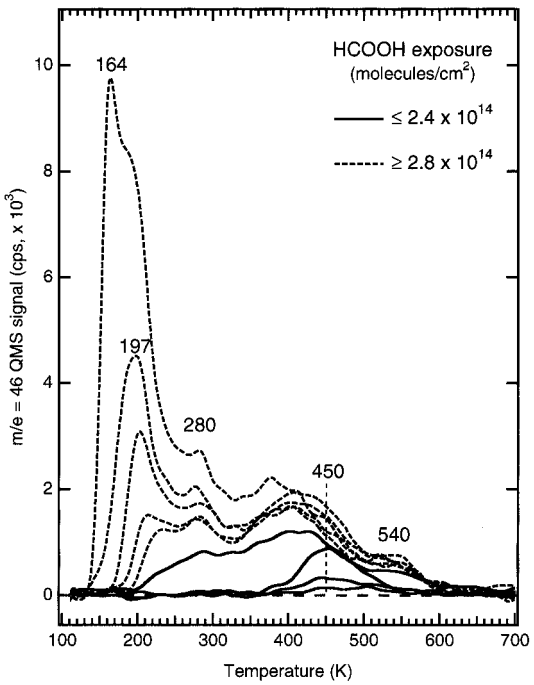

Figure 4. HCOOH TPD from HCOOH adsorbed on TiO_2(110). HCOOH exposures were 0.2, 0.5, 1.1, 2.4, 2.8, 3.2, 4.1, 5.2, and 7.3×10^{14} molecules/cm^2.

Although it was mentioned above that a small amount of CO_2 was observed in TPD, a significant $m/e = 44$ signal was detected over much of the HCOOH exposure regime explored in these experiments. Comparison of the desorption traces for $m/e = 44$ with those for HCOOH ($m/e = 46$) suggests that most of the $m/e = 44$ signal resulted from QMS cracking of HCOOH. However, some of the $m/e = 44$ signal was due to CO_2 desorption, as can be seen by comparing the $m/e = 44$ and 46 signals obtained from HCOOH adsorbed on TiO_2(110) at 300 K (Figure 5). To facilitate comparison of the $m/e = 44$ and 46 signals, the $m/e = 46$ signal was scaled so that the leading edges of the two desorption signals traced each other. With this normalization in mind, a proportion of $m/e = 44$ signal registered between 380 and 600 K (the shaded region of Figure 5) was probably due to CO_2 desorption, while the rest of the $m/e = 44$ signal was due to HCOOH desorption. A further comparison of the $m/e = 44$ and 46 signals with the $m/e = 28$ signal indicates that some of the $m/e = 28$ signal between 300 and 500 K was due to HCOOH and/or CO_2 desorption but that virtually all the $m/e = 28$ signal above 500 K was due to CO desorption. Comparison of the amount of CO relative to that of CO_2 (based on the QMS signals) indicates that formate decomposition to CO dominated on TiO_2(110).

Analysis of the adsorption and decomposition of HCOOH on TiO_2(110) with HREELS was attempted with a moderate

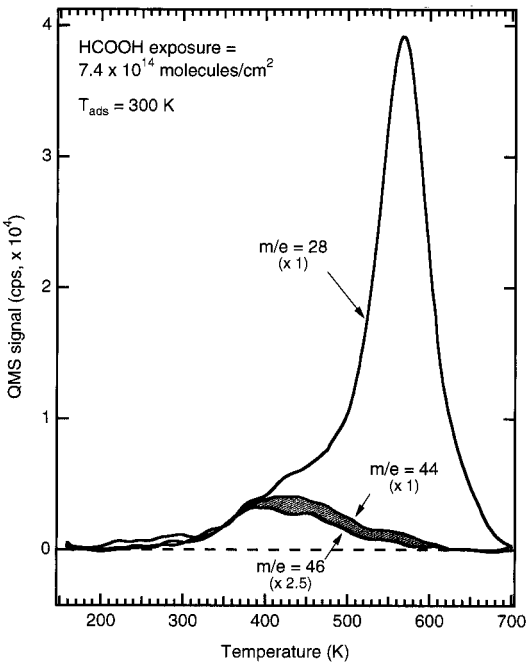

Figure 5. TPD spectra from a 7.4×10^{14} molecules/cm^2 exposure of HCOOH on TiO_2(110) adsorbed at 300 K. The crystal was cooled to 160 K before beginning TPD.

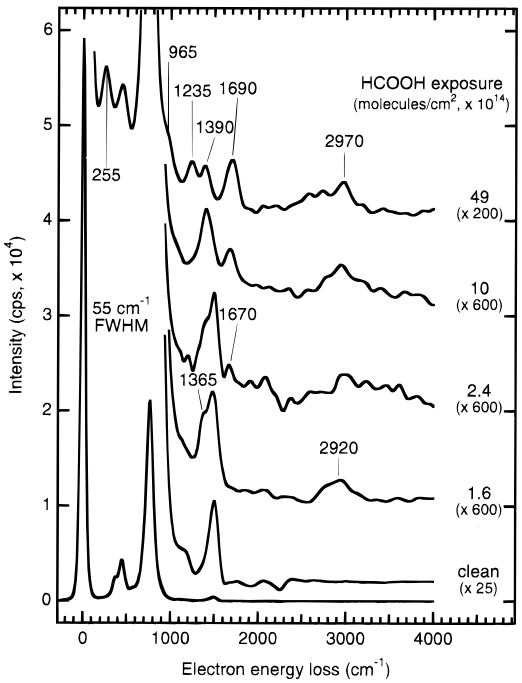

Figure 6. Fourier deconvoluted HREELS spectra of various HCOOH exposures on TiO_2(110) at 110 K. The beam energy was 8.8 eV. Each trace resulted from a fresh HCOOH exposure.

degree of success. In general, Fourier deconvolution of the multiple phonon losses in the HREELS spectra of TiO_2(110)[18] with adsorbed HCOOH required a high signal-to-noise level in the raw data. Although the elastic peak count rates were high ($\geq 5 \times 10^4$ cps) for the clean surface, they attenuated significantly upon adsorption of HCOOH, resulting in lower signal-to-noise and less than desired quality in some of the deconvoluted data. Identification of weak modes (O−H stretches, for example) was difficult. Also, positive- and negative-going remnants of the first and second sets of multiply phonon losses, respectively, signified less than ideal deconvolution of the data. Therefore, the focus of the following two figures will be on those modes that were clearly discernible after Fourier deconvolution and that revealed information regarding the decomposition of formic acid and formate on TiO_2(110).

Figure 6 shows Fourier deconvoluted HREELS data from various HCOOH exposures on TiO_2(110) at 110 K. The lower trace shows the clean surface spectrum after deconvolution of the multiple phonon modes. As discussed in a previous work,[18] positive- and negative-going remnants of the deconvolution process were present in the first and second sets of multiple phonon losses, respectively. More than likely, these features in the deconvoluted spectrum were the result of less than perfect spectrometer tuning and/or sample positioning. The spectral region above 2500 cm^{-1} was, for the most part, free of these deconvolution remnants. After exposure of the surface to 1.6×10^{14} molecules/cm^2 of HCOOH at 110 K, losses at 1365 and 2920 cm^{-1} were clearly observed in the deconvoluted spectrum. Since no apparent loss intensity was present in the ν(C═O) stretching region for the parent molecule (at about 1650−1720 cm^{-1}), the 1365 and 2920 cm^{-1} losses were assigned to the ν_s(OCO) and ν(CH) modes of adsorbed formate.[16,21,22,24] A weak loss at about 3600 cm^{-1} could be due to the ν(OH) mode of a surface hydroxyl, as was observed for the dissociation of trace amounts of water on TiO_2(110).[18] However, its weak intensity prevented a definite assignment. Although the spectral quality degraded significantly after adsorption of 2.4×10^{14} molecules/cm^2 HCOOH, a weak loss at 1670 cm^{-1} reflected the presence of molecular HCOOH adsorption on TiO_2(110) at 110 K. The 1670 cm^{-1} loss increased in intensity with higher HCOOH exposures such that after a 1.0×10^{15} molecules/cm^2 exposure pronounced losses were present in the HREELS spectrum at 1405, 1670, and 2950 cm^{-1}. After a 4.9×10^{15} molecules/cm^2 exposure losses were present at 255, 965, 1235, 1390, 1690, 2575−2720, and 2970 cm^{-1}. These features can be assigned to the various modes of multilayer formic acid.[22] Note that one major difference between the HREELS spectrum after a 1.0×10^{15} molecules/cm^2 exposure (≥ 3 layers) from that after a 4.9×10^{15} molecules/cm^2 exposure (>10 layers) is the absence of the 1235 cm^{-1} loss in the former spectrum assigned to the ν(C−O) mode of HCOOH. This difference suggests that the structure of thin HCOOH ice layers on TiO_2(110) is different from that of thick layers and may relate to the formation of formic anhydride at the interface between chemisorbed and physisorbed HCOOH (see discussion of TPD results above).

Figure 7 shows Fourier deconvoluted HREELS data taken after heating a 1.0×10^{15} molecules/cm^2 exposure of HCOOH on TiO_2(110) to various temperatures. The 110 K spectrum (the same as that shown in Figure 6) changed slightly after annealing the surface to 200 K. This temperature, according to Figure 4, was sufficient to desorb multilayer HCOOH but not all of the 205 K TPD state. The 1675 cm^{-1} loss (ν(C═O) mode) was absent after heating the surface to 250 K, indicating that all (detectable) molecular HCOOH had either desorbed or decomposed. Therefore, after heating to 250 K, the surface was populated with formate species and bridging hydroxyl groups (some molecular water was also present based on TPD results). The bridging OH groups were difficult to detect with HREELS after heating to 250 K. This may be due to a weak dynamic dipole for the O−H stretch of this species, especially compared to the terminal O−H group, which has been detected previously by HREELS on TiO_2(110),[18] or it may indicate that these OH species were hydrogen-bonded to other species (e.g., formates or water molecules). A weak loss at 3610 cm^{-1} was detected after heating to 300 K, indicative of an O−H stretching mode. The presence of this mode after heating to 300 K may have resulted from the desorption of formic acid and/or water molecules that freed bridging hydroxyls from hydrogen-bonding interactions. Evidence for formic acid and water desorption in this temperature range was presented above. Attenuation of

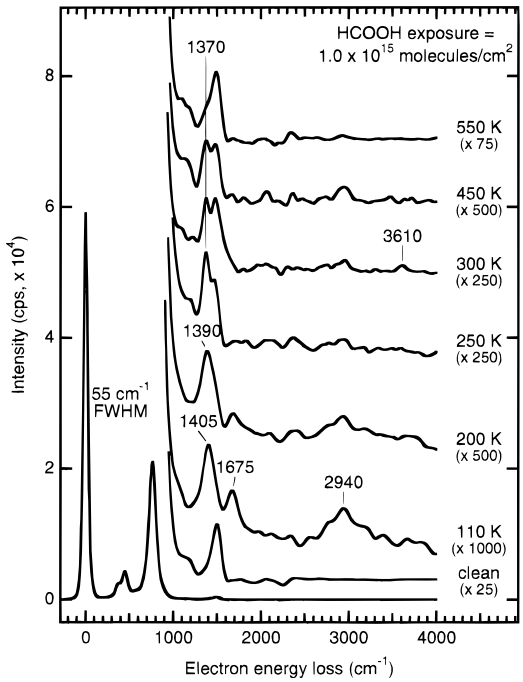

Figure 7. Fourier deconvoluted HREELS spectra of a 1.0×10^{15} molecules/cm^2 HCOOH exposure on TiO_2(110) at 110 K followed by heating to various temperatures. The beam energy was 8.8 eV. Each spectrum was recorded at 110 K and resulted from a fresh HCOOH exposure.

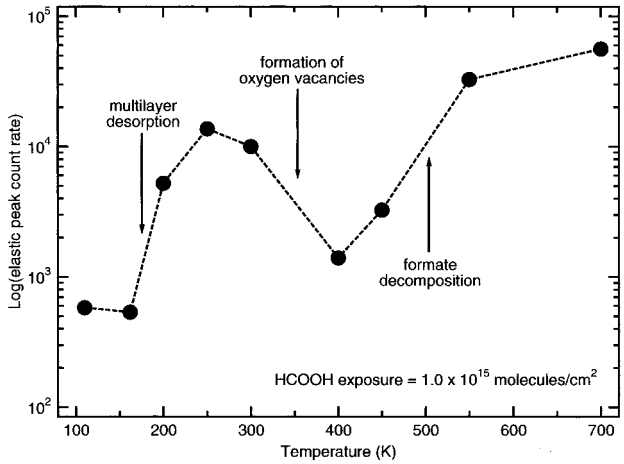

Figure 8. Logarithmic plot of the HREELS elastic peak count rate after heating a 1.0×10^{15} molecules/cm^2 exposure of HCOOH on TiO_2(110) to various temperatures. Count rates were obtained after recooling to 110 K.

the 1370 cm^{-1} loss, which is the main signature of formate, also suggests formic acid desorption occurred after heating to 300 K. The 3610 cm^{-1} was absent after heating to 450 K, whereas the 1370 cm^{-1} loss was unchanged. The 1370 cm^{-1} loss decreased in intensity after heating to 550 K owing to the decomposition of formate. (A weak loss at about 2350 cm^{-1} in some of the spectra of Figure 7 was due to background CO_2 adsorption during acquisition of the HREELS data.)

Analysis of the elastic peak count rates as a function of the preheating temperature for a multilayer exposure of HCOOH on TiO_2(110) revealed something interesting about the surface during HCOOH decomposition. Figure 8 shows the log of the elastic peak count rates obtained for a 1.0×10^{15} molecules/cm^2 exposure of HCOOH on TiO_2(110) at 110 K and after heating to various temperatures (some of which are shown in Figure 7). Between 110 and 165 K the HREELS elastic peak count rate was below 1 kilocount/s (kcps) because the surface was covered with about four layers of HCOOH ice. However, the elastic peak count rate increased by an order of magnitude when the multilayer was desorbed by heating above 165 K. Desorption of additional formic acid by heating to 250 K resulted in a further increase of the elastic peak count rate to above 10 kcps. After heating to this temperature, the surface was populated primarily with formate species and presumably bridging hydroxyl groups. Under these conditions, Onishi and co-workers observed an ordered (2×1) formate adlayer by low-energy electron diffraction (LEED) and scanning tunneling microscopy (STM).[4,5] As the surface was heated above 300 K, the elastic peak intensity dropped sharply by over an order of magnitude and did not significantly recover until the formate layer was decomposed by heating to 500 K and above. Although surface formate was stable in the temperature regime around 400 K, the surface appeared disordered and less reflective to the 8.8 V HREELS electron beam than for annealing temperatures at or below 300 K. This is consistent with observations by Onishi et al. that the (2×1) LEED pattern was not stable above 350 K.[4] TPD indicates that two processes occurred in the temperature regime between 300 and 400 K, both of which relate to the surface hydroxyls formed from formic acid decomposition to formate. First, some hydroxyls and formate species combined, resulting in parent formic acid desorption (Figure 4). Second, the remainder of the hydroxyl groups combined to form water (Figure 2). Although the first process should somewhat disorder the adlayer by depleting the (2×1) formate coverage, it should not significantly decrease the HREELS elastic peak count rate. The second process is expected to have a more significant effect on the structure of the surface if these hydroxyl groups comprise the acid proton from the dissociated formic acid molecule and a lattice oxygen, presumably a bridging surface atom. Reaction of two such hydroxyls to form water should leave an oxygen vacancy on the surface.

3.2. Creation of Oxygen Vacancies. TPD experiments were performed utilizing oxygen-18 in order to verify that lattice oxygen atoms were abstracted by the hydrogen atoms deposited on the surface during formic acid decomposition to formate. For these experiments the TiO_2(110) surface was isotopically enriched with ^{18}O by oxidizing at 820 K in greater than 5×10^{-7} Torr $^{18}O_2$ for 5 min. (The effective $^{18}O_2$ pressure at the crystal was probably about an order of magnitude greater than this because a direction doser was used.) Examination with +SSIMS prior to adsorption of formic acid revealed that virtually all of the surface probed by the 500 eV Ar^+ beam was $Ti^{18}O_2$ (Figure 9a). A similar +SSIMS scan taken after two successive TPD experiments to 750 K, each with a $HC^{16}O^{16}OH$ exposure of 7.3×10^{14} molecules/cm^2, revealed a more intense signal at $m/e = 64$, indicating that a significant amount of $^{16}O-^{18}O$ exchange occurred between the formic acid adlayer and the ^{18}O-enriched surface (Figure 9b). (The exchange process was also apparent after a single TPD experiment but was much more apparent after two.) The increased ^{16}O concentration at the surface was not the result of oxygen exchange between the $Ti^{16}O_2$ bulk and the $Ti^{18}O_2$ surface during the TPD experiment because oxygen atom bulk diffusion is kinetically limited under these conditions.[25] Exchange between the bulk and the surface was also invalidated because annealing the "before" surface of Figure 9a at 750 K did not alter the +SSIMS spectrum. Therefore, the presence of ^{16}O in the ^{18}O-enriched surface was due to isotopic exchange with the $HC^{16}O^{16}OH$ adlayer. Figure 10 shows TPD results from the decomposition of approximately one monolayer (2.8×10^{14} molecules/cm^2) of formic acid on the ^{18}O-enriched TiO_2(110) surface. In the top half of Figure 10 TPD spectra of $H_2{}^{16}O$ (dashed line) and $H_2{}^{18}O$ (solid line) reveal that over half the total water

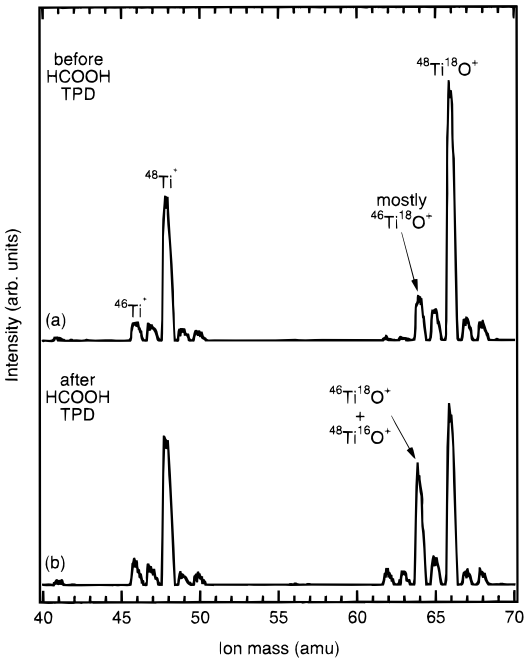

Figure 9. +SSIMS (0.5 kV, 3.5 nA/cm^2) spectra of the ^{18}O-enriched TiO_2(110) surface before (a) and after (b) two successive TPD experiments each with a $HC^{16}O^{16}OH$ exposure of 7.3×10^{14} molecules/cm^2.

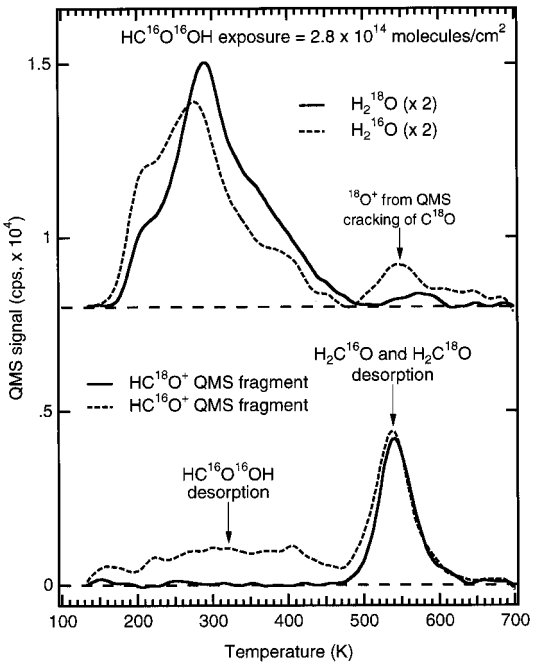

Figure 10. TPD of water (m/e = 18 and 20), of the HCO^+ QMS cracking fragments (m/e = 29 and 31), and from the decomposition of $HC^{16}O^{16}OH$ on the ^{18}O-enriched TiO_2(110) surface. The $HC^{16}O^{16}OH$ exposure was of 2.8×10^{14} molecules/cm^2.

desorption signal below 500 K contained ^{18}O. The presence of ^{18}O in the water TPD of Figure 10 strongly suggests that bridging ^{18}OH groups condensed to form water, leaving an oxygen vacancy on the surface. The remaining water TPD signal (containing ^{16}O) resulted from water dosed (as an impurity) with formic acid or from condensation of adsorbed formic acid molecules as shown in reaction 1. Since previous studies of $H_2{}^{16}O$ on the ^{18}O-enriched TiO_2(110) surface indicate that water does not exchange oxygen atoms with this surface,[26] the desorption of $H_2{}^{18}O$ was not associated with this water impurity. Note also, based on comparison of the $HC^{16}O^+$ (dashed line) and $HC^{18}O^+$ (solid line) QMS cracking fragments in the bottom half of Figure 10, that adsorbed $HC^{16}O^{16}OH$ molecules do not exchange oxygen atoms with the ^{18}O-enriched surface. This applies both to molecularly desorbed formic acid (desorbing below 250 K) and recombinatively desorbed formic acid (desorbing between 250 and 450 K). In contrast, extensive incorporation of ^{18}O into the formaldehyde product at 540 K occurred (to be discussed).

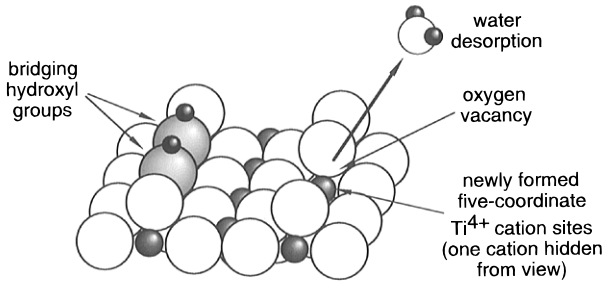

Figure 11. Schematic model for the creation of oxygen vacancies on TiO_2(110) by combination of bridging hydroxyl groups to form water.

The formation of oxygen vacancies by the condensation of bridging hydroxyl groups has previously been proposed by Kim and Barteau[11] for formic acid decomposition on anatase powder, by this author[6] for formic acid decomposition on TiO_2(100), and more recently by Gamble and co-workers[27] for ethanol decomposition on TiO_2(110). On the basis of these studies, it appears that bridging hydroxyl groups on TiO_2 are somewhat labile with respect to water formation and the creation of oxygen vacancy sites by water desorption. The presence of oxygen vacancies from formic acid decomposition on TiO_2(110) presumably caused the significant drop in the HREELS elastic peak intensity between 300 and 400 K (Figure 8). This assertion is supported by previous HREELS work by Eriksen and Egdell,[28] which showed that the TiO_2(110) surface became less reflective to specular scattering of low-energy electrons when oxygen vacancies were present. If the formate coverage at 250 K was near 0.5 monolayer (ML) (2.6×10^{14} molecules/cm^2), as suggested by the STM and LEED results of Onishi et al.,[4,5] then the number of oxygen vacancies resulting from abstraction of the lattice oxygen to produce water could be close to 0.25 ML (1.3×10^{14} sites/cm^2). The actual number was probably less than 0.25 ML, since a significant amount of HCOOH recombinative desorption also occurred below 400 K.

The exact nature of these oxygen vacancy sites is not obvious from the data in this study. Simplistically, the condensation of two bridging hydroxyl groups to form a water molecule is an acid−base process and not a redox process, so the newly exposed cations are not Ti^{3+} sites. Instead, each water molecule formed should generate two five-coordinate Ti^{4+} atoms that share a single oxygen vacancy site, as illustrated in Figure 11. With a surface coverage of these sites near 1.3×10^{14} sites/cm^2, it is possible that two such sites could form adjacent to each other, resulting in lower coordination Ti^{4+} cations, a prerequisite for formaldehyde production from formate in the absence of reduced cation centers.[7] Therefore, the presence of this high surface concentration of defect sites should have a significant effect on the chemistry of formate on TiO_2(110), especially if a number of these sites are low in coordination.

3.3. Formic Acid and Formate Decomposition Mechanisms. Since carbon monoxide and water were the major TPD products observed for formic acid decomposition on TiO_2(110) in this study, the overall stoichiometry for their production can be represented by reaction 2:

$$HCOOH \rightarrow CO + H_2O \qquad (2)$$

It is generally accepted that formate is the stable intermediate resulting from the first step in the HCOOH decomposition on

most oxide surfaces. The HREELS results discussed above (Figures 7 and 8) support this for HCOOH on TiO_2(110). Therefore, reaction 2 can be expanded to

$$HCOOH + O^{2-}_{(lattice)} \rightarrow HCOO^{-}_{(a)} + OH^{-}_{(lattice)} \quad (3)$$

$$HCOO^{-}_{(a)} + OH^{-}_{(lattice)} \rightarrow CO + H_2O + O^{2-}_{(lattice)} \quad (4)$$

where the designation "lattice" refers, for argument's sake, to a bridging two-coordinate O^{2-} site, and "a" refers to an adsorbed species at a five-coordinate Ti^{4+} site. (For simplicity, gaseous products receive no designation.) For HCOOH decomposition on TiO_2(110), reaction 3 is somewhat straightforward, but there are two problems with reaction 4. First, reaction 4 embeds two independent reaction processes: the formation and desorption of water, which occurred below 500 K, and the decomposition of formate, which occurred in this study predominantly above 500 K. Based on the TPD results discussed above, the water product resulted from condensation of two bridging hydroxyl groups formed at two-coordinate O^{2-} sites (lattice sites):

$$2OH^{-}_{(lattice)} \rightarrow H_2O + O^{2-}_{(lattice)} + vac \quad (5)$$

where "vac" refers to an oxygen vacancy site (see Figure 11). The water product contains an oxygen atom from the surface and not from the formate species. This process was nearly complete before the onset of formate decomposition (reaction 6). Therefore, the desorption of water

$$HCOO^{-}_{(a)} \rightarrow CO + OH^{-}_{(a)} \quad (6)$$

and the decomposition of formate to yield CO are not directly linked.

Contemplation of reactions 5 and 6 might lead one to expect that the hydroxyl groups formed in reaction 6, which presumably were adsorbed at five-coordinate Ti^{4+} sites, could react together and form water, with the remaining oxygen atom filling the vacancy site shown in reaction 5. In this way, formate decomposition could be described as a dehydration process. The first problem with reaction 4 would then be resolved by rewriting reactions 3 and 4 as

$$2HCOOH + 2O^{2-}_{(lattice)} \rightarrow 2HCOO^{-}_{(a)} + 2OH^{-}_{(lattice)} \quad (7)$$

$$2OH^{-}_{(lattice)} \rightarrow H_2O + O^{2-}_{(lattice)} + vac \quad (8)$$

occurring below 500 K and

$$2HCOO^{-}_{(a)} \rightarrow 2CO + 2OH^{-}_{(a)} \quad (9)$$

$$2OH^{-}_{(a)} \rightarrow H_2O + O^{2-}_{(a)} \quad (10)$$

$$O^{2-}_{(a)} + vac \rightarrow O^{2-}_{(lattice)} \quad (11)$$

occurring above 500 K. The summation of reactions 7−11 gives

$$2HCOOH \rightarrow 2CO + 2H_2O \quad (12)$$

However, this set of reactions does not address the second problem with reaction 4, which is that very little water was produced during formate decomposition. Instead, formaldehyde appeared to be the dominant hydrogen-containing product of formate decomposition with formic acid (from disproportionation of formates) and acetylene as additional hydrogen-containing species. The absence of appreciable amounts of water above 500 K would appear to invalidate reaction 10. The formaldehyde and carbon dioxide products could be produced according to reaction 13:

$$2HCOO^{-}_{(a)} + vac \rightarrow CO_2 + H_2CO + O^{2-}_{(lattice)} \quad (13)$$

Despite the apparent simplicity of this reaction, an ensemble of vacancies is probably required in order for this bimolecular reaction to occur.[7] This requirement might explain why CO_2 and H_2CO were minor products compared to CO. Oxygen vacancies created by water formation may play a key role in the reactions of other intermediates on TiO_2 surfaces. For example, Gamble and co-workers[27] recently observed ethylene formation from the decomposition of ethoxy groups at oxygen vacancies sites on TiO_2(110). These authors proposed that the vacancy sites were formed by the reaction of protons (from dissociation of the O−H bond of ethanol) with lattice oxygen atoms to form water below 400 K.

In contrast to this complex chemistry on TiO_2(110), the decomposition of formic acid on MgO(100) follows a straightforward dehydration mechanism. Formic acid decomposes on MgO(100) to a formate and a surface proton.[24] Both these species remain on the surface until above 500 K at which point CO and H_2O are liberated in concomitant TPD peaks with no other decomposition products observed.[14] The major differences between formic acid chemistry on MgO(100) and TiO_2(110) appear to be the relative ease with which lattice oxygen atoms are abstracted by protons (to form water) on TiO_2(110) and the subsequent influence of resulting oxygen vacancies on formate decomposition.

The remaining data in this study will focus on an additional complexity in the decomposition of formate on TiO_2(110), that of oxygen exchange with the lattice.

3.4. Oxygen Exchange between Adsorbed Formate and the Surface. As was observed for the {110}-microfaceted surface of TiO_2(100),[6] oxygen atoms in adsorbed formate species readily scrambled with lattice oxygen atoms in the TiO_2(110) surface. Scrambling into the formaldehyde (Figure 10) and carbon monoxide products was observed in TPD by adsorbing $HC^{16}O^{16}OH$ on an ^{18}O-enriched TiO_2(110) surface. The exchange of oxygen atoms between the surface and adsorbed formate was also observed with +SSIMS in the temperature-programmed mode. In Figure 12, the $HC^{16}O^{+}$ and $HC^{18}O^{+}$ SSIMS signals were followed during temperature-programmed heating of a 7.3×10^{14} molecules/cm^2 exposure of $HC^{16}O^{16}$-OH on the ^{18}O-enriched TiO_2(110) surface. The $HC^{16}O^{+}$ signal was the largest SSIMS signal from the multilayer. This signal dropped significantly as the multilayer desorbed (between 160 and 200 K) but remained significant above 250 K (only formate on the surface), indicating that both formate and molecular formic acid contribute to the SSIMS HCO^{+} signal. The $HC^{16}O^{+}$ signal decreased at a slower rate as the surface was heated between 210 and 400 K, presumably because of formic acid recombinative desorption (see Figure 4), but attenuated to zero between 400 and 600 K as result of formate decomposition. The $HC^{18}O^{+}$ signal remained relatively constant, and near zero, in the temperature region between 200 and 400 K but increased between 400 and 500 K before following the $HC^{16}O^{+}$ signal to zero at 600 K. The incorporation of lattice oxygen into formate is better perceived by examining the ratio of the $HC^{18}O^{+}$ and $HC^{16}O^{+}$ signals as shown in the inset of Figure 12. This ratio was constant, and near zero, between 110 and 400 K but began increasing as the temperature exceeded 400 K. (The ratio is meaningless above 600 K because both the numerator and denominator attenuated to zero owing to formate decomposition.) The data in Figure 12 indicate that exchange of lattice oxygen into formate occurred at a detectable rate at approximately the same temperature as that for the onset of CO desorption in TPD (see below).

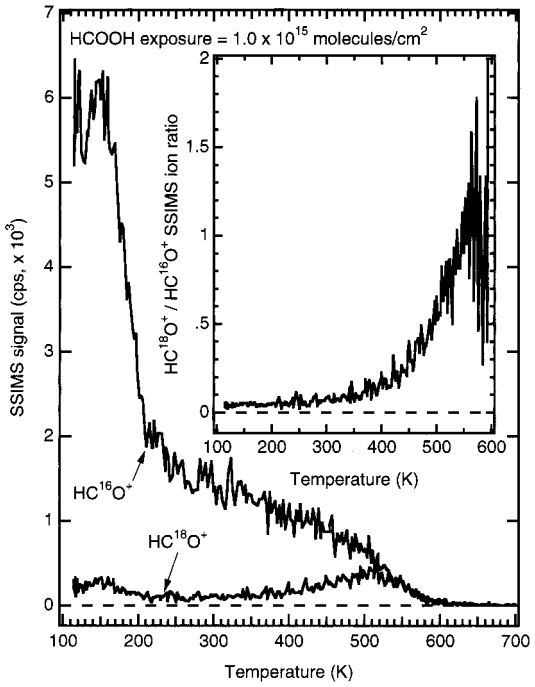

Figure 12. Temperature-programmed +SSIMS (0.5 kV, 3.5 nA/cm^2) of the $HC^{16}O^+$ and $HC^{18}O^+$ ion signals from a 7.3×10^{14} molecules/cm^2 exposure of $HC^{16}O^{16}OH$ on the ^{18}O-enriched TiO_2(110) surface. The inset shows the ratio of the $HC^{18}O^+$ and $HC^{16}O^+$ signals as a function of temperature.

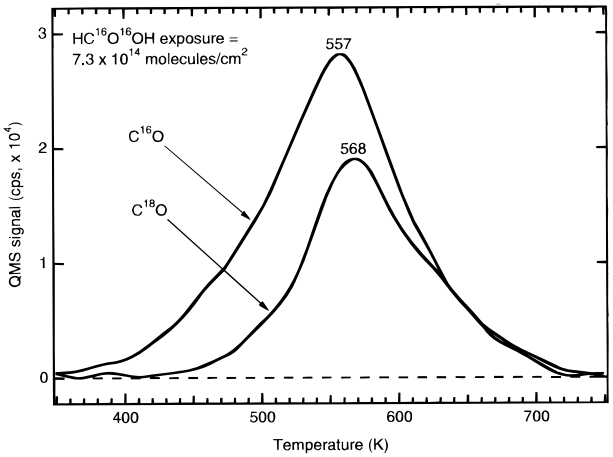

Figure 13. Non-line-of-sight TPD of $C^{16}O$ and $C^{18}O$ (m/e = 28 and 30, respectively) resulting from a 7.3×10^{14} molecules/cm^2 $HC^{16}O$-^{16}OH exposure on the ^{18}O-enriched TiO_2(110) surface at 110 K.

3.5. Formate Decomposition and Oxygen Exchange Kinetics. Although exchange of lattice oxygen (^{18}O) with ^{16}O-formate was detectable by +SSIMS at about 400 K, the evolution of ^{18}O in the major formate TPD product, carbon monoxide, did not occur at the same rate as that for ^{16}O, the oxygen isotope of the parent species. This is shown by comparing the $C^{16}O$ (m/e = 28) and $C^{18}O$ (m/e = 30) TPD signals from the adsorption of $HC^{16}O^{16}OH$ on the ^{18}O-enriched TiO_2(110) surface (Figure 13). To discriminate against contributions to these signals from other desorption products such as formic acid and formaldehyde, the TPD experiment was performed in a non-line-of-sight geometry. Under this condition, contributions from formic acid (by comparison with the parent signals) and from formaldehyde (by comparison with the HCO^+ QMS fragment signals) were negligble. Relative contributions from cracking of carbon dioxide were also smaller than in the line-of-sight geometry. Figure 13 shows that the TPD spectra for $C^{16}O$ and $C^{18}O$ from $HC^{16}O^{16}OH$ decomposition on the ^{18}O-enriched TiO_2(110) surface do not track each other. The $C^{18}O$ TPD peak temperature was at least 10 K higher, and the peak was narrower than the $C^{16}O$ TPD peak. Also, the onset for the desorption of $C^{18}O$ was about 50 K higher than that for $C^{16}O$. The onset for $C^{18}O$ desorption (slightly above 400 K) matched the temperature at which +SSIMS detected oxygen exchange between the surface and formate.

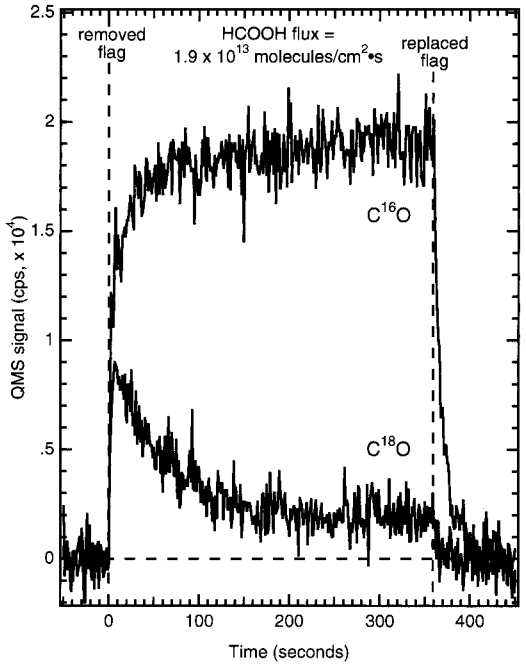

Figure 14. $C^{16}O$ and $C^{18}O$ QMS signals (m/e = 28 and 30, respectively) during exposure of $HC^{16}O^{16}OH$ to the ^{18}O-enriched TiO_2(110) surface at 555 K. The signals were obtained with the crystal in a non-line-of-sight geometry with respect to the QMS.

To examine the kinetics of the incorporation of lattice oxygen (^{18}O) into the CO product of formate decomposition, a series of isothermal reaction experiments were performed, similar to those described by Onishi and co-workers.[3,4] Figure 14 illustrates this methodology for a reaction temperature of 555 K. The ^{18}O-enriched TiO_2 surface was positioned in front of a directional doser and flag assembly in such a way that a non-line-of-sight geometry existed between the crystal face and the QMS. For reasons mentioned above, this geometry ensured that other desorbing products would not significantly contribute to the m/e values for $C^{16}O$ and $C^{18}O$. Additionally, the formic acid flux was maintained at a low level (1.9×10^{13} molecules cm^{-2} s^{-1}) to prevent detection of any unreacted molecules. With the flag positioned between the crystal and the doser and with a constant $HC^{16}O^{16}OH$ flux passing through the doser, the crystal was ramped to the desired temperature. At time "zero" the flag was rotated out of the formic acid beam and the QMS registered the resulting carbon monoxide signals as a function of time. The $C^{16}O$ and $C^{18}O$ signals immediately rose after the flag was removed, indicating formic acid decomposition on the ^{18}O-enriched TiO_2(110) surface. Since the $^{18}O_2$ treatment used to prepare the ^{18}O-enriched surface resulted in almost complete replacement of ^{16}O with ^{18}O in the near surface region (see Figure 9), the $C^{16}O$ signal near time zero was the result of decomposition events that did not involve oxygen exchange. However, a significant portion of the decomposing formic acid and formate species exchanged oxygen atoms with the surface prior to carbon monoxide desorption, as can be seen by the $C^{18}O$ signal at time zero. The $C^{18}O$ signal decayed with time as the surface became depleted of ^{18}O and repleted with ^{16}O (see Figure 9). The flag was replaced in front of the crystal after sufficient time for a steady reaction to have been established, and the surface was then replenished with ^{18}O for the next experiment by heating in $^{18}O_2$.

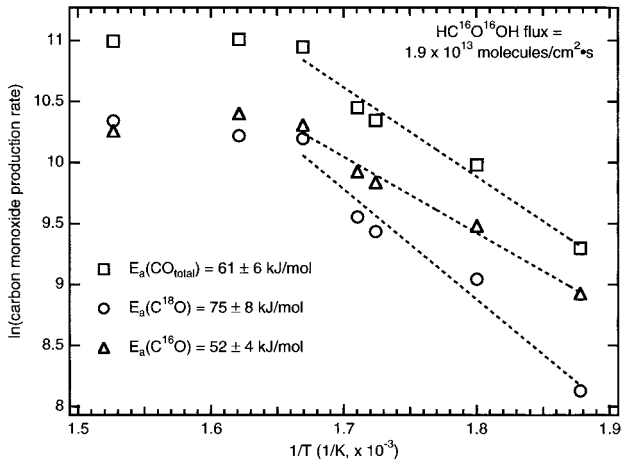

Figure 15. Arrhenius plot for the instantaneous rates of carbon monoxide production during decomposition $HC^{16}O^{16}OH$ on the ^{18}O-enriched TiO_2(110) surface.

In Figure 15, the instantaneous (time zero) rates of $C^{16}O$, $C^{18}O$, and total carbon monoxide are plotted versus $1/T$ for various reaction temperatures between 530 and 655 K. In this plot the rates of carbon monoxide production were obtained from the slopes of the first-order least-squares fits of the integrated signals in the first few seconds after the flag was rotated out of the beam. Least-squares analysis of the natural log of these rates versus inverse temperature yielded good fits to the data between 530 and 600 K (1.88 and 1.67×10^{-3} K^{-1}). The rates of carbon monoxide production were constant above 600 K because the rate of formate decomposition became limited by the flux of formic acid. The activation barrier for the production of $C^{18}O$ (75 ± 8 kJ/mol) was 23 kJ/mol higher than that for $C^{16}O$ (52 ± 4 kJ/mol). (Errors were based on standard deviations obtained from the fit.) The lower activation barrier is associated with the unimolecular decomposition of formate on TiO_2(110). The higher barrier either indicates a separate formate decomposition pathway that involves lattice oxygen atoms or an exchange process between formate (or a formate decomposition intermediate) and the surface.

By the combination of the $C^{16}O$ and $C^{18}O$ integrated signals, an overall activation barrier of 61 ± 6 kJ/mol was obtained. This value may have little meaning, however, because it was obtained by combining the rates of two apparently independent chemical processes. Nevertheless, a second kinetic analysis was undertaken to compare the activation energy for the instantaneous rate of total carbon monoxide production with that of a steady-state rate. For this analysis the $C^{16}O$ and $C^{18}O$ signals were added and integrated with respect to time. The integrated signals were then fit by first-order least-squares analysis, and the steady-state reaction rates were obtained from the slopes of the integrated total carbon monoxide yields versus time. This analysis yielded an activation barrier of 59 ± 4 kJ/mol, which compares well with that obtained from the instantaneous rate of total carbon monoxide production in Figure 15 (61 ± 6 kJ/mol).

The activation energy for formate decomposition on TiO_2(110) to carbon monoxide obtained in this study is about half that obtained by Onishi et al.[3,4] (120 ± 10 kJ/mol) from a similar kinetic analysis. These authors found support for their kinetic value for CO production from formate decomposition by comparison with a 107 kJ/mol activation energy obtained by Munuera[8] for formic acid decomposition on rutile powder. However, Munuera observed two regimes for CO production from formic acid decomposition, one occurring above 623 K (with the 107 kJ/mol activation energy) and one observed between 423 and 523 K with an activation energy of 43.9 kJ/mol. This latter value compares more closely with the activation barrier obtained in this study for $C^{16}O$ production (52 ± 4 kJ/mol) from $HC^{16}O^{16}OH$ decomposition on the ^{18}O-enriched TiO_2-(110) surface between 530 and 600 K.

4. Conclusions

The decomposition of formic acid on TiO_2(110) consists of a complex set of chemical processes that cannot adequately be described in terms of a simple dehydration mechanism. These complex processes include (1) creation of oxygen vacancy sites by the reaction of the acid protons (from formic acid decomposition to formate) with lattice oxygen atoms to form water, (2) facile oxygen exchange between the surface and adsorbed formate species that occurs during formate decomposition, and (3) at least two independent formate decomposition processes, one of which may involve the oxygen vacancies created during water desorption to create the minor TPD products (H_2CO, CO_2, C_2H_2) observed in this study. These findings also show that TiO_2 surfaces participate in the reactions of simple organic molecules to a greater extent than providing surface cation and anion sites that facilitate unimolecular or bimolecular processes.

Acknowledgment. This work was supported by the U.S. Department of Energy, Office of Basic Energy Sciences, Division of Materials Science.

References and Notes

(1) Onishi, H.; Aruga, T.; Egawa, C.; Iwasawa, Y. *Surf. Sci.* **1988**, *193*, 33.
(2) Kim, K. S.; Barteau, M. A. *Langmuir* **1990**, *6*, 1485.
(3) Onishi, H.; Aruga, T.; Iwasawa, Y. *J. Am. Chem. Soc.* **1993**, *115*, 10460.
(4) Onishi, H.; Aruga, T.; Iwasawa, Y. *J. Catal.* **1994**, *146*, 557.
(5) Onishi, H.; Iwasawa, Y. *Chem. Phys. Lett.* **1994**, *226*, 111.
(6) Henderson, M. A. *J. Phys. Chem.* **1995**, *99*, 15253.
(7) Idriss, H.; Lusvardi, V. S.; Barteau, M. A. *Surf. Sci.* **1996**, *348*, 39.
(8) Munuera, G. *J. Catal.* **1970**, *18*, 19.
(9) Groff, R. P.; Manogue, W. H. *J. Catal.* **1983**, *79*, 462.
(10) Trillo, J. M.; Munuera, G.; Criado, J. M. *Catal. Rev.* **1972**, *7*, 51.
(11) Kim, K. S.; Barteau, M. A. *Langmuir* **1988**, *4*, 945.
(12) Columbia, M. R.; Thiel, P. A. *J. Electroanal. Chem.* **1994**, *369*, 1.
(13) Vohs, J. M.; Barteau, M. A. *Surf. Sci.* **1986**, *176*, 91.
(14) Peng, X. D.; Barteau, M. A. *Catal. Lett.* **1990**, *7*, 395.
(15) Ludviksson, A.; Zhang, R.; Campbell, C. T.; Griffiths, K. *Surf. Sci.* **1994**, *313*, 64.
(16) Xu, C.; Goodman, D. W. *J. Chem. Soc., Faraday Trans.* **1995**, *91*, 3709.
(17) Henderson, M. A. *Surf. Sci.* **1994**, *319*, 315.
(18) Henderson, M. A. *Surf. Sci.* **1996**, *355*, 151.
(19) Hugenschmidt, M. B.; Gamble, L.; Campbell, C. T. *Surf. Sci.* **1994**, *302*, 329.
(20) Erley, W.; Sander, D. *J. Vac. Sci. Technol. A* **1989**, *7*, 2238.
(21) Truong, C. M.; Wu, M.-C.; Goodman, D. W. *J. Chem. Phys.* **1992**, *97*, 9447.
(22) Dilara, P. A.; Vohs, J. M. *J. Phys. Chem.* **1993**, *97*, 12919.
(23) Gercher, V. A.; Cox, D. F. *Surf. Sci.* **1994**, *312*, 106.
(24) Petrie, W. T.; Vohs, J. M. *Surf. Sci.* **1991**, *259*, L750.
(25) Henderson, M. A. *Surf. Sci.* **1995**, *343*, L1156.
(26) Henderson, M. A. *Langmuir* **1996**, *12*, 5093.
(27) Gamble, L.; Jung, L. S.; Campbell, C. T. *Surf. Sci.* **1996**, *348*, 1.
(28) Eriksen, S.; Egdell, R. G. *Surf. Sci.* **1987**, *180*, 263.